JOURNAL OF COMPUTATIONAL PHYSICS **100**, 322–334 (1992)

A Hybrid Spectral Method for the Three-Dimensional Numerical Modelling of Nonlinear Flows in Shallow Seas

R. W. LARDNER AND Y. SONG

Mathematics Department, Simon Fraser University, Burnaby, British Columbia, Canada

Received July 13, 1990; revised May 8, 1991

A spectral method employing eddy-viscosity eigenfunctions is used to solve the full three-dimensional nonlinear hydrodynamic equations for the numerical computation of flows caused by tides or meteorological forcing. An explicit finite element method is developed to compute the nonlinear advective terms and an explicit treatment of bottom friction is used. This leads to a rapidly convergent expansion and relatively few eigenfunctions are required to obtain accurate solutions. An Arakawa B-grid is used in the horizontal directions and leapfrog time-stepping. The eigenfunctions are computed at the beginning of the program, for an arbitrary spatial dependence of eddy viscosity, using the SLEIGN subroutine. Several model problems have been used to test the accuracy, stability, and computational efficiency of the method.

1. INTRODUCTION

Numerical studies of the three-dimensional motion of the sea under the influence of wind and tide have in recent years been made by several authors using a number of different approaches. Some of the most successful of these approaches make use of expansions of the two horizontal components of fluid velocity in terms of a set of basis functions of the vertical coordinate. By this means the three-dimensional equations are reduced to a set of two-dimensional modal equations for the coefficients in these velocity expansions.

The use of a basis of "eddy-viscosity eigenfunctions" for this purpose was first proposed by Heaps [1, 2] to solve the linearized three-dimensional tidal equations. The significant advantage of this particular basis is that the modal equations are uncoupled. Since Heaps employed analytic eigenfunctions, his use of the method was restricted to problems with simple eddy-viscosity profiles and to linear bottom friction. Subsequently, extensions of the method have been made by Davies and Furnes [3] to include nonlinear friction and by Davies [4] and Furnes [5] to more general eddy-viscosities. A general approach is described by Davies [6, 7].

A more general Galerkin method was developed by Davies and Owen [8] for the linearized model and by Davies [9] for the fully nonlinear equations. In these papers basis sets consisting of cosine functions, Chebychev polynomials, and Gram–Schmidt orthogonalized polynomials (equivalent to shifted Legendre polynomials) were used. Davies [7] later combined the Galerkin method with use of a basis set of eddy viscosity eigenfunctions.

The rate of convergence of the expansions in terms of eddy viscosity eigenfunctions was found by Davies [4, 7] to be relatively slow, requiring typically 15–20 basis functions to obtain the desired accuracy. Much more rapid convergence is obtained using Chebychev or Legendre polynomials [9], but the disadvantage of these basis sets is that the modal equations are coupled even in the linear approximation. Using eddy-viscosity eigenfunctions, the equations are coupled only through the nonlinear terms. A later modification of the method that significantly accelerates the convergence was proposed for the linearized equations by Lardner [10]. With this modification it was found in one model problem that only 4–5 eddy-viscosity eigenfunctions were required to give the same accuracy as had previously [4] been obtained with 20–25 eigenfunctions. The rate of convergence is comparable to that obtained using B-splines [11] or Chebychev polynomials [9] and has the advantage over these approaches of uncoupling the linear modal equations. An equivalent modification has also been proposed by Davies [12].

In the present paper this modified eddy-viscosity eigenfunction method is extended to the nonlinear hydrodynamical equations. An explicit method is used to represent the nonlinear bottom friction and an explicit finite element method is used for the nonlinear advective terms (compared to the explicit time-splitting technique used by Davies [9]). This treatment of the bottom friction does not add significantly to the CPU requirements of the algorithm, but we have found, as did Davies, that computation of the advective terms is by far the most expensive part of the algorithm, in our case increasing the CPU requirements by a factor of more than 3. The finite element technique is the most effective method we have found for minimizing this cost.

0021-9991/92 $5.00

Most of the finite difference schemes that have been developed for hydrodynamical modelling, including the algorithms based on the spectral method, have been based on an Arakawa C-grid [13]. While this choice of grid has the advantage of providing natural centred-difference approximations to most of the dominant terms and of minimizing numerical dispersion at short wavelengths, it does lead to certain difficulties for some three-dimensional algorithms. The first of these, pointed out by Jamart and Ozer [14], is the occurrence of spurious numerical boundary layers unless the Coriolis terms are treated by what these authors term "wet points only" averaging. A second, and probably more serious, disadvantage of the C-grid that arises for spectral methods is that it is necessary to use the same basis functions at all grid points if the four-point average for the Coriolis terms is not to couple the modal equations. The basis set of eddy-viscosity eigenfunctions are independent of position only if the eddy viscosity function has the same vertical profile at all points, apart from an overall scaling factor, and this is a severe restriction for a water body with widely varying parameters such as depth or bottom roughness.

Because of these problems, Lardner and Song [15] have examined the feasibility of using alternative Arakawa grids for which the two velocity components are computed at the same spatial points. They have concluded that the Arakawa B-grid is about as accurate and computationally efficient as the C-grid, and it does not suffer from the problems described above. Consequently, in this paper a B-grid scheme is used and is found to work satisfactorily. It is worth noting that a B-grid has also recently been used by James [16].

An important feature of the finite element approach used for the advective terms is that these terms are computed at each grid point directly from the velocity fields and are then resolved into their modal amplitudes. This only requires the eigenfunctions at that one grid point. This approach never requires horizontal derivatives of the eigenfunctions or eigenfunctions at more than one point at a time and thus preserves the advantage of the B-grid over the C-grid.

In Section 2 we write down the basic equations for the spectral method, using eddy-viscosity eigenfunctions as basis functions and in Section 3 some details of the numerical scheme are given. In Section 4 numerical results are given for a number of problems designed to test the accuracy of the algorithm and bounds on its stability are determined.

2. BASIC EQUATIONS

(a) *Hydrodynamical Equations*

We use xyz as Cartesian coordinates with the z-axis pointing vertically upwards and the xy-plane occupying the undisturbed position of the water surface. The integrated equation of continuity and the horizontal momentum equations for a homogeneous sea, including the nonlinear terms, but neglecting shear in the horizontal and the direct influence of tide-generating forces, and making the usual hydrostatic pressure approximation, may be written as

$$\frac{\partial \zeta}{\partial t}+\frac{\partial p}{\partial x}+\frac{\partial q}{\partial y}=0 \tag{1}$$

$$\frac{\partial u}{\partial t}+u\frac{\partial u}{\partial x}+v\frac{\partial u}{\partial y}+w\frac{\partial u}{\partial z}-fv=-g\frac{\partial \zeta}{\partial x}+\frac{\partial}{\partial z}\left(N\frac{\partial u}{\partial z}\right) \tag{2}$$

$$\frac{\partial v}{\partial t}+u\frac{\partial v}{\partial x}+v\frac{\partial v}{\partial y}+w\frac{\partial v}{\partial z}+fu=-g\frac{\partial \zeta}{\partial y}+\frac{\partial}{\partial z}\left(N\frac{\partial v}{\partial z}\right), \tag{3}$$

where the volume transports and vertical component of velocity are given by

$$p=\int_{-h}^{\zeta} u\,dz, \qquad q=\int_{-h}^{\zeta} v\,dz \tag{4}$$

$$w=-\frac{\partial}{\partial x}\int_{-h}^{z} u\,dz-\frac{\partial}{\partial y}\int_{-h}^{z} v\,dz. \tag{5}$$

The notation used in these equations is as follows:

$h(x, y)$	water depth
$\zeta(x, y, t)$	surface elevation at time t
$u(x, y, z, t)$, $v(x, y, z, t)$	horizontal velocity components
$w(x, y, z, t)$	vertical velocity component
$p(x, y, t)$, $q(x, y, t)$	depth integrated volume transports
f	Coriolis parameter
$N(x, y, z, t)$	vertical eddy viscosity
g	acceleration due to gravity.

Equations (1)–(3) require boundary conditions on the sea surface and at the sea bed. The surface conditions, evaluated at $z=\zeta$, are

$$\rho N\frac{\partial u}{\partial z}=\tau_x, \qquad \rho N\frac{\partial v}{\partial z}=\tau_y, \tag{6}$$

We denote the eigenpairs by $\{\phi_j(\sigma), \lambda_j : j = 0, 1, 2, \ldots\}$, where the lowest eigenpair is $\lambda_0 = 0$, $\phi_0(\sigma) = 1$. For a general eddy-viscosity, it is necessary to compute the other eigenpairs numerically. For this purpose we have used the subroutine SLEIGN [20].[1] This routine has also been used for similar computations by Kuzmic [21]. We assume the eigenfunctions are normalized so that

$$\int_0^1 \phi_j(\sigma)^2 \, d\sigma = 1. \tag{22}$$

The eigenfunctions then form an orthonormal system, and in particular, orthogonality with ϕ_0 implies that

$$\int_0^1 \phi_j(\sigma) \, d\sigma = 0, \qquad j \geq 1. \tag{23}$$

In general, these eigenpairs depend on x and y, and also on t if the eddy-viscosity is time dependent. For the general case they must be determined numerically, and if N varies in a general way with t this usually makes the method impractical, since the eigenfunctions must be re-determined at each time step for all horizontal points. Consequently, we shall from now on restrict to the case when N is independent of t.[2] The eigenfunctions can then be determined at the beginning of the computation and, although this can be quite expensive, it only has to be done once.

We now expand W in terms of the eigenfunctions:

$$W(\sigma) = c_0 + \sum_{j \geq 1} c_j \phi_j(\sigma). \tag{24}$$

In view of the orthonormality of the eigenfunctions, the coefficients in the expansion (24) are given by

$$\begin{aligned} c_0 &= \int_0^1 W(\sigma) \, d\sigma \equiv \bar{W}, \\ c_j &= \int_0^1 W(\sigma) \, \phi_j(\sigma) \, d\sigma, \qquad j \geq 1. \end{aligned} \tag{25}$$

Using the definition of W, we have that $c_0 = \bar{U} - \bar{V}$ and from Eq. (15) it then follows that

$$c_0 = \bar{U} - H(S - B) \int_0^1 \frac{\sigma(1-\sigma)}{N(\sigma)} \, d\sigma. \tag{26}$$

Integrating the differential equation (18) from $\sigma = 0$ to $\sigma = 1$ and using the boundary conditions (19), we obtain an equation for c_0. This is equivalent to the usual depth-averaged momentum equation, and it is in fact more convenient to use this equation in the latter form, which can be obtained more directly by integrating Eq. (10):

$$\frac{\partial \bar{U}}{\partial t} + if\bar{U} + g\left(\frac{\partial \zeta}{\partial x} + i\frac{\partial \zeta}{\partial y}\right) = R_0, \tag{27}$$

where

$$R_0 = H^{-1}(S - B) + \int_0^1 F_{NL} \, d\sigma. \tag{28}$$

Multiplying the differential equation (18) by $\phi_j(\sigma)$, integrating from $\sigma = 0$ to $\sigma = 1$ and using the boundary conditions (19) and (13), we obtain a system of differential equations for the coefficients c_j:

$$\frac{\partial c_j}{\partial t} + \alpha_j c_j = R_j. \tag{29}$$

where $\alpha_j = h^{-2}\lambda_j^2 + if$ and the right side is given by

$$R_j = R_j^{NL} + R_j^{v} + (H^{-2} - h^{-2}) \, \lambda_j^2 c_j \tag{30}$$

with

$$R_j^{NL} = \int_0^1 F_{NL} \phi_j \, d\sigma \tag{31}$$

and

$$R_j^{v} = \int_0^1 \left[-\frac{\partial V}{\partial t} - ifV \right] \phi_j \, d\sigma = -\frac{\partial I}{\partial t} - ifI_j, \tag{32}$$

provided the eigenfunctions are time-independent, where

$$\begin{aligned} I_j &\equiv \int_0^1 V(\sigma) \, \phi_j(\sigma) \, d\sigma \\ &= \frac{1}{\lambda_j^2} \{HS\phi_j(1) - HB\phi_j(0)\}. \end{aligned} \tag{33}$$

In the numerical solution of Eq. (27) and (29) the terms on the right sides are treated explicitly. The final small nonlinear term on the right of Eq. (30) can quite easily be accommodated on the left side of (29), but the coefficients on the left than become time-dependent and this adds significantly to the cost of the algorithm.

In order to obtain initial conditions for the system (27) and (29), we assume the motion starts from some given

---

[1] We are indebted to Dr. Paul Bailey for his help in supplying us with a recent version of this program.

[2] The method can readily be extended to the case when the eddy viscosity has the form

$$N(x, y, \sigma, t) = N_1(x, y, \sigma) \, N_2(t)$$

that is, at any point N has a similar profile for all t.

where U_l is the value of $U(\sigma)$ at node l and so on. The various terms in Eq. (39) are then approximated as

$$\int_0^1 \sigma U_\sigma \phi_j\, d\sigma = \sum_{l=1}^{L-1} (U_{l+1} - U_l)\, S_{lj}^{(1)}$$

$$\int_0^1 \tilde{w} U_\sigma \phi_j\, d\sigma = \sum_{l=1}^{L-1} \frac{\tilde{w}_{l+1} - \tilde{w}_l}{\Delta\sigma} (U_{l+1} - U_l)\, S_{lj}^{(2)} + \sum_{l=1}^{L-1} \tilde{w}_l (U_{l+1} - U_l)\, S_{lj}^{(3)}$$

$$\int_0^1 [uU_x + vU_y]\, \phi_j\, d\sigma = \sum_{l=1}^{L-1} \{(u_l U_{x,l} + v_l U_{y,l})\, S_{lj}^{(4)} + (u_{l+1} U_{x,l+1} + v_{l+1} U_{y,l+1})\, S_{lj}^{(6)} + (u_l U_{x,l+1} u_{l+1} U_{x,l} + v_l U_{y,l+1} + v_{l+1} U_{y,l})\, S_{lj}^{(5)}\},$$

where

$$S_{lj}^{(1)} = \frac{1}{\Delta\sigma} \int_{\sigma_l}^{\sigma_{l+1}} \sigma \phi_j\, d\sigma,$$

$$S_{lj}^{(2)} = \frac{1}{\Delta\sigma} \int_{\sigma_l}^{\sigma_{l+1}} (\sigma - \sigma_l)\, \phi_j\, d\sigma,$$

$$S_{lj}^{(3)} = \frac{1}{\Delta\sigma} \int_{\sigma_l}^{\sigma_{l+1}} \phi_j\, d\sigma,$$

$$S_{lj}^{(4)} = \int_{\sigma_l}^{\sigma_{l+1}} \left(\frac{\sigma - \sigma_{l+1}}{\Delta\sigma}\right) \phi_j\, d\sigma,$$

$$S_{lj}^{(5)} = \int_{\sigma_l}^{\sigma_{l+1}} \left(\frac{\sigma_{l+1} - \sigma}{\Delta\sigma} \frac{\sigma - \sigma_l}{\Delta\sigma}\right) \phi_j\, d\sigma,$$

$$S_{lj}^{(6)} = \int_{\sigma_l}^{\sigma_{l+1}} \left(\frac{\sigma - \sigma_l}{\Delta\sigma}\right)^2 \phi_j\, d\sigma.$$

It remains to compute $\tilde{w}$ from Eq. (14). We first use a trapezoidal approximation:

$$\int_0^{\sigma_l} u\, d\sigma = \tfrac{1}{2} \Delta\sigma \sum_{k=1}^{l-1} [u_{k+1} + u_k],$$

$$\int_0^{\sigma_l} v\, d\sigma = \tfrac{1}{2} \Delta\sigma \sum_{k=1}^{l-1} [v_{k+1} + v_k].$$

Then $\tilde{w}_l$ can be constructed recursively as

$$\tilde{w}_1 = 0,$$

$$\tilde{w}_{l+1} = \tilde{w}_l - \frac{1}{2} \Delta\sigma \left\{ \frac{\partial}{\partial x} [H(u_{l+1} + u_l)] + \frac{\partial}{\partial y} [H(v_{l+1} + v_l)] \right\}.$$

We note that the nonlinear terms are computed here directly from the three-dimensional velocity fields. This avoids the appearance of horizontal derivatives of the eigenfunctions. Since eigenfunctions at only one horizontal grid point are used at any one time, the advantages of the B-grid are not forfeited.

4. NUMERICAL RESULTS

(a) *One-Dimensional Channel Flow*

It is not easy to find exact solutions of the nonlinear equations with which to test the accuracy of numerical algorithms. One such solution, however, occurs for the steady wind-driven flow in a channel of constant depth. If, for such a case of uni-directional flow, one makes the approximation $H \approx h$, the advective terms become identically zero and the only nonlinearity is the bottom friction. In this case, for constant eddy-viscosity, the final steady solution can be found analytically.

With these approximations, Eq. (1) and (10) reduce, for steady flow, to

$$\frac{\partial p}{\partial x} = 0, \qquad \frac{\partial}{\partial \sigma}\left(N \frac{\partial u}{\partial \sigma}\right) = gh^2 \frac{\partial \zeta}{\partial x},$$

where $p = h \int_0^1 u\, d\sigma = h\bar{u}$, and the boundary conditions (11) [illegible]

$$N \frac{\partial u}{\partial \sigma} = hS \qquad \text{on} \quad \sigma = 1,$$

$$N \frac{\partial u}{\partial \sigma} = hB \equiv h(\kappa_1 + \kappa_2 |u|) u \qquad \text{on} \quad \sigma = 0.$$

We take the channel to be closed at its ends, so that the boundary conditions are $p = 0$. Therefore $p = 0$ for all x. Then the solution of these equations is

$$u(\sigma) = \tfrac{1}{2} u(0)(3\sigma^2 - 6\sigma + 2) + (Sh/4N)(3\sigma^2 - 2\sigma)$$

$$\partial\zeta/\partial x = (6Nu(0) + 3Sh)/2gh^2,$$

where the bottom velocity is given by

$$u(0) = (\varepsilon/2\kappa_2 h)\{\kappa_1 h + 3N - \sqrt{(\kappa_1 h + 3N)^2 + 2\varepsilon\kappa_2 h^2 S}\}$$

with $\varepsilon = 1$ if $S \geq 0$ and $\varepsilon = -1$ if $S < 0$.

For the numerical solution, the dynamical equations (1), (27), and (29) are solved from an initial state of rest until the steady flow is reached. In this case, these equations simplify to

$$\frac{\partial\zeta}{\partial t}+\frac{\partial p}{\partial x}=0,\qquad \frac{\partial\bar{u}}{\partial t}+g\frac{\partial\zeta}{\partial x}=H^{-1}(S-B),$$

$$\frac{\partial c_j}{\partial t}+h^{-2}\lambda_j^2 c_j=\frac{h\phi_j(0)}{\lambda_j^2}\frac{\partial B}{\partial t}$$

while the velocity is obtained from Eq. (35) as

$$u(\sigma)=\bar{u}+\frac{hS}{2N}\left(\sigma^2-\frac{1}{3}\right)-\frac{hB}{2N}\left\{(1-\sigma)^2-\frac{1}{3}\right\}+\sum_{j\geqslant 1} c_j\phi_j(\sigma).$$

The algorithm described in Sections 2 and 3 is easily adapted to these simplified equations by setting the Coriolis parameter equal to zero and bypassing computation of the y-component of velocity. All nonlinear terms are suppressed except for the bottom friction. Some typical results are given in Table I. In these computations, the values of the various parameters where chosen as $h=65$ m, $\Delta x=47{,}059$ m, $\tau=360$ s, $N=0.065$ m^2/s, and $g=9.81$ m/s^2. Six eigenfunctions were used in the calculations and the length of the channel was 16 horizontal grids.

Table I gives the exact solution in the last column and in the adjacent columns the computed solutions at three points spaced along the channel. The velocity is given at the surface, mid-depth, and bottom in each case. Results are given for several combinations of values of the linear and quadratic friction coefficients κ_1 and κ_2. It can be seen that the numerical results are quite accurate, even for very small drag coefficients and that the algorithm remains stable for both small and large values of these coefficients.

(b) *Rectangular Sea with Constant Eddy Viscosity*

In order to test the algorithm for the full three-dimensional nonlinear hydrodynamic equations, we have made use of the simplified storm-surge model of the North Sea used by Davies [4, 7–9] and also several other investigators [e.g., 10, 14]. The model region consists of a closed rectangular sea of dimensions 400 km in the x-direction and 800 km in the y-direction, with grid spacings $\Delta x=400/9$ km and $\Delta y=800/17$ km. Figure 1 shows the B-grid used for this region. The depth is taken uniformly as 65 m. The sea is initially in a state of equilibrium and starting at $t=0$ is subjected to a constant surface shear stress in the negative y-direction, with values $\tau_x=0$, $\tau_y=-1.5$ N/m^2. The values of the other parameters (all in MKS units) are $\rho=1025$, $N=0.065$, $g=9.81$, and $f=1.22\times10^{-4}$. A time step $\tau=360$ s was used. These parameters have been chosen to be identical to those used in earlier work [8, 9] so that comparisons can be made. Comparable results to many of those reported below have also been obtained with a shallower depth of 35 m.

TABLE I

Computed and Exact Velocities in cm/s for Steady Wind-Driven Flow in a Channel with Different Values of Linear and Quadratic Friction Coefficients

		Computed solution at points			Exact
κ_1 and κ_2	Level	(2)	(8)	(15)	solution
$\kappa_1=0.002$	S	−40.54	−40.56	−40.55	−40.53
$\kappa_2=0.05$	M	8.11	8.09	8.10	8.11
	B	8.07	8.07	8.07	8.07
$\kappa_1=0.002$	S	−41.99	−42.01	−42.00	−41.99
$\kappa_2=0.015$	M	7.74	7.73	7.74	7.75
	B	10.98	10.98	10.98	10.98
$\kappa_1=0$	S	−43.60	−43.60	−43.60	−43.61
$\kappa_2=0.015$	M	7.35	7.36	7.35	7.34
	B	14.22	14.23	14.22	14.22
$\kappa_1=0$	S	−45.66	−45.12	−45.44	−45.78
$\kappa_2=0.005$	M	6.91	7.43	7.12	6.80
	B	18.65	18.99	18.78	18.57

Note. Velocities are given at the surface, mid-point, and bottom of the water column.

TABLE II

Computed Velocity Profiles in cm/s after 30 h for the Linearized Equations

Velocity		(2, 2)	(8, 10)	(5, 15)
Surface	u	−9.86	−14.82	−10.56
	v	−39.68	−35.03	−35.95
Mid-level	u	5.51	1.12	4.78
	v	3.47	7.67	6.91
Bottom	u	9.96	7.28	9.38
	v	8.51	10.97	10.63
Surface	u	−9.85	−14.85	−10.58
	v	−39.72	−34.97	−35.98
Mid-level	u	5.52	1.11	4.78
	v	3.47	7.72	6.92
Bottom	u	9.95	7.27	9.41
	v	8.56	11.03	10.72

Note. Profiles are given at the three grid points (2, 2), (8, 10), and (5, 15) (see Fig. 1). The upper part of the table provides the results from the present algorithm and the lower part from the implicit algorithm of [15].

to ensure that the algorithm remains stable for large friction. Typical results are shown in Table V for several values of κ_1 and κ_2. We have experimented with large values of κ_1 and κ_2 and small eddy viscosity to determine the stability limits of the algorithm. Using the time step of 360 s, the algorithm remains stable for all physically realistic values of these parameters. For example, with $N = 0.065$, stability is maintained up to and beyond $\kappa_2 = 0.2$ when $\kappa_1 = 0$ and up to $\kappa_2 = 0.02$ when $\kappa_1 = \kappa_2$. With $\kappa_1 = 0$ and $\kappa_2 = 0.002$, stability is maintained for $N \geqslant 0.001$, while for $\kappa_1 = 0.002$ and $\kappa_2 = 0$, it is maintained for $N \geqslant 0.004$. Figure 2 shows the regions of stability and instability in the N-κ_2 plane in the case when $\kappa_1 = 0$.

(c) *Rectangular Sea with Variable Eddy Viscosity*

To further test the algorithm, a three-dimensional nonlinear problem with a more realistic eddy viscosity function

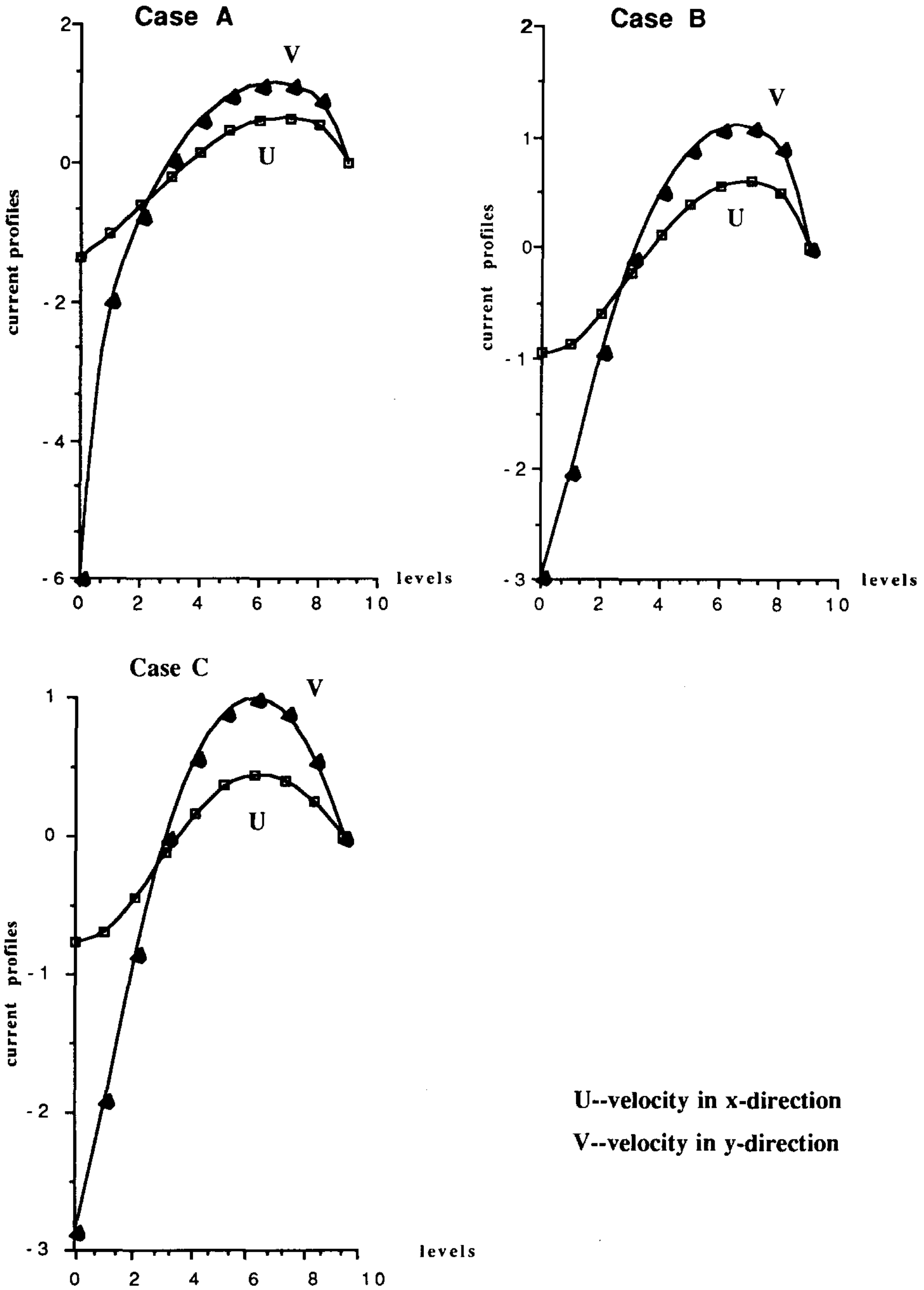

FIG. 4. The velocity profile as a function of vertical coordinate, 75 h after the onset of the wind, at the centre of the rectangle (point A in Fig. 2), for the three eddy viscosity functions shown in Fig. 3, and for the no-slip bottom condition.

was used. Three cases of variable viscosity were considered, again following Ref. [9] for the sake of comparison, as shown in Fig. 3. The water depth was taken as 65 m, and the thicknesses d_1 and d_2 of the surface and bottom layers were taken as 11 m. Within these boundary layers N is assumed to vary linearly with the vertical coordinate, while N is constant through the rest of the water column. The values used for the parameters in the three cases were:

$$\begin{aligned}
\text{Case A: } & N_s = 0.013\ \mathrm{m^2/s},\ N_m = 0.065\ \mathrm{m^2/s},\\
& N_b = 0.013\ \mathrm{m^2/s},\\
\text{Case B: } & N_s = 0.117\ \mathrm{m^2/s},\ N_m = 0.065\ \mathrm{m^2/s},\\
& N_b = 0.013\ \mathrm{m^2/s},\\
\text{Case C: } & N_s = 0.117\ \mathrm{m^2/s},\ N_m = 0.065\ \mathrm{m^2/s},\\
& N_b = 0.065\ \mathrm{m^2/s}.
\end{aligned}$$

In this case, again for the sake of comparison with [9], a no-slip boundary condition (8) was used. The algorithm must then be modified as indicated in Section 2(c). Figure 4 shows the two components of velocity as a function of vertical coordinate 75 h after the onset of the wind at the centre of the rectangle for the three eddy viscosity functions. These were computed using six eigenfunctions. The most striking feature of these figures is the sensitivity of the near-surface velocities to the value of N_s. The no-slip condition prevents the bottom velocity from being as strongly affected by N_b, although the effect on the velocity gradient is noticeably affected.

In Fig. 5 we have reproduced the figure given by the continuous curves in Fig. 4 of [9] corresponding to Case A. This was computed using four Chebychev or shifted Legendre Polynomials. There is substantial, but not complete, agreement between this figure and that in Fig. 4a. The differences are again probably ascribable to the numerical boundary layers.

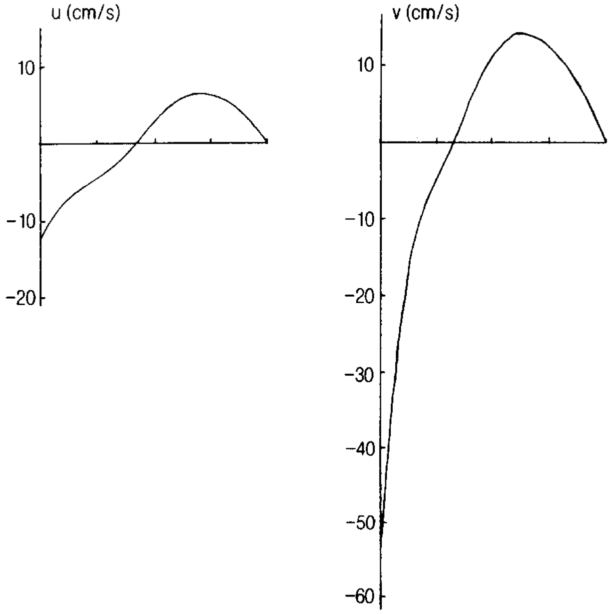

FIG. 5. The profiles of u and v computed by Davies [6] for the same case as shown in Fig. 4a.

5. SUMMARY

The principal features of the algorithm described in this paper can be summarized as follows:

(a) It is directed towards solving the fully nonlinear hydrodynamic equations as usually approximated for flows in shallow seas of uniform density, with an eddy-viscosity model of turbulence.

(b) The numerical approach to the dependence on the vertical coordinate is a spectral method of Galerkin type, using eddy-viscosity eigenfunctions as the basis set. The advantage of this basis is that the modal equations are not coupled through the linear terms, which are the dominant ones in most cases.

(c) By an appropriate modification of the velocity before expansion, the method provides a uniformly convergent series that converges rapidly and for which truncations exactly satisfy the surface and bottom boundary conditions.

(d) The cost of this modification is an explicit treatment of bottom friction. This certainly imposes a stability restriction which, however, has not turned out to be a serious limitation in the problems examined.

(e) The advective terms are computed directly from the three-dimensional velocity fields using a finite element method. This is the most efficient means we have found for this part of the algorithm, which is by far the most expensive, requiring two-thirds of the total CPU time. This cost may, however, be reduced by computing these terms every several steps.

(f) The numerical approach to the horizontal variations is via a staggered B-grid, which has some advantages over the more usual C-grid when a spectral method is used.

(g) A leapfrog method is used for the time-stepping, in which the surface elevation and the velocity are computed on alternate half-steps. Account is taken of the stiffness of the system of modal equations.

(h) The algorithm permits arbitrary horizontal and vertical variation of eddy viscosity without any loss of computational efficiency.

The performance of the algorithm has been tested satisfactorily on a number of problems (see Section 4). For steady wind-driven flow in a channel with nonlinear bottom